Imaging profiles of light intensity in the near field: applications to phase-shift photolithography

Joanna Aizenberg, John A. Rogers, Kateri E. Paul, and George M. Whitesides

We describe a method of imaging the intensity profiles of light in near-field lithographic experiments directly by using a sensitive photoresist. This technique was applied to a detailed study of the irradiance distribution in the optical near field with contact-mode photolithography carried out by use of elastomeric phase masks. The experimental patterns in the photoresist determined by scanning electron microscopy and atomic force microscopy were compared with the corresponding theoretical profiles of intensity calculated by use of a simple scalar analysis; the two correlate well. This comparison makes it possible to improve the theoretical models of irradiance distribution in the near field. Analysis of the images highlights issues in the experimental design, provides a means for the optimization of this technique, and extends its application to the successful fabrication of test structures with linewidths of ~50 nm.

OCIS codes: 050.5080, 110.5220, 110.0110.

1. Introduction

Near-field optics offers an approach to deep submicrometer photolithography.[1–4] The quality of the lithography is determined primarily by the irradiance distribution. Optimization of lithographic methods that operate in the near field can therefore be accelerated by a quantitative understanding of the intensity profiles of light in this region. Intensive computational efforts have focused on an accurate analysis of the irradiance distribution in the near field.[5–8] In practice, it is often the case that not all variables that contribute to the formation of the light-intensity profiles are properly understood or completely modeled theoretically, and these models have necessarily been approximate.

In this paper we illustrate a simple procedure for imaging the irradiance distribution in the near field experimentally in terms of the topology of features in a photoresist. Different photosensitive materials have been used previously to characterize the optical probe in near-field microscopy[9] and to act as recording media for holograms.[10–11] The resist used in our study makes it possible to image the irradiance distribution directly because the thickness of the resist remaining after exposure and development is thickest where the intensity of light is greatest.[12] The topology of the developed resist is thus related to the irradiance profile qualitatively, although the detailed form of the relation has not been established quantitatively. We believe that this procedure provides a sensitive method for imaging details of the optical near field, and that it is a very useful tool for testing and improving theoretical models of the intensity distribution in the near field.

We focused our efforts on near-field photolithography by using an elastomeric phase mask. The essentials of this method—which is capable of generating ~90-nm-wide features with broadband (λ = 330–460-nm) incoherent light—have been described previously.[4–5] This technique combines certain advantages of conformable-contact photolithography by using amplitude masks[1,2,8] and phase-shift lithography.[13–17] We show that the new imaging method provides a reliable near-field image that can be reconciled with theory. On the basis of these calculations, we propose that the major mode of action of the elastomeric mask is as a phase mask but that distortions in the relief of the mask in contact with the surface of the photoresist may produce amplitude modulation as well. Imaging these intensity profiles is an important component of a program to optimize contact-mode near-field phase-shifting photolithography and to extend its

The authors are with the Department of Chemistry, Harvard University, 12 Oxford Street, Cambridge, Massachusetts 02138-2902.

Received 15 September 1997; revised manuscript received 24 November 1997.

0003-6935/98/112145-08$15.00/0

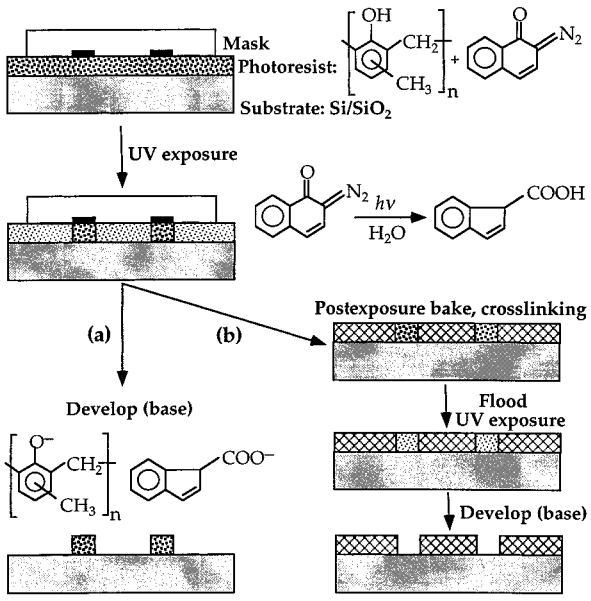

Fig. 1. Schematic illustration of the processing of the AZ 5200 series photoresists with an amplitude mask in the (a) conventional and (b) image-reversal modes.

ability to fabricate structures to the 50-nm domain. Although we did not explicitly work with noncontact phase and amplitude masks, the procedures described here should work for them as well.

2. Experiment

Elastomeric phase masks were prepared as described previously[18] by the casting and curing of polydimethylsiloxane (PDMS, Sylgard 184, Dow Corning) against patterned rigid masters. A 10:1 liquid prepolymer reaction mixture of Si elastomer to its curing agent (A:B) was used. The masters were Si (100) wafers (Silicon Sense, Inc.) with surfaces that had been patterned with a photoresist film (Shipley, Model 1805) of an appropriate relief structure by conventional photolithography. The thicknesses of the photoresist films and the corresponding depths of the surface relief of the phase masks were 0.5 μm ($\sim\pi$ phase shift for wavelengths emitted by a Hg lamp).[4]

The procedure for imaging the irradiance distribution in the optical near field consisted of several steps. First, a 0.5-μm film of AZ 5206 photoresist (Hoechst) was spun onto a Si wafer. The elastomeric phase mask was then allowed to come into conformal contact with the photoresist. The resist was exposed through the mask by use of a standard mask aligner (Karl Suss, Model MJB3 UV400) equipped with a Hg lamp (emission peaks at 365, 405, and 436 nm). The mask was removed from the surface, and the photoresist was soft baked for 1.5 min at 120 °C, flood-UV exposed for 2 min, and developed in a base (Hoechst) for 1.5 min (Fig. 1). By varying the time of exposure through the phase mask from 0.2 to 10 s, we determined that a 2.25-s exposure provided conditions in which the photoresist acted with a response to the integrated irradiation that was close to linear (Figs. 2 and 3).

The topology of the photoresist surface that was modified according to the irradiance distribution in the near field was examined with a JEOL Model JSM-6400 scanning electron microscope operating at 15 keV and a Topometrix atomic force microscope (AFM).

To study the effect of distortions in elastomeric masks[19] on the quality of the lithographic experiment, we prepared PDMS masks of increasing stiffness (reaction mixtures of the Si elastomer to its curing agent from 20:1 to 5:1) and different thicknesses (2–8 mm). For each mask we generated and characterized structures in the photoresist (Shipley, Model 1805), produced as described previously.[4–5]

3. Results and Discussion

A. Choice of a Photosensitive Polymer System

The most important characteristic of a photoresist that is appropriate for imaging intensity profiles is its sensitivity to the variations in the integrated dose of radiation. We used AZ 5200 photoresist (Hoechst) because of its high sensitivity and its unique ability to work in both positive and image-reversal modes (Fig. 1). This resist is composed of a base resin (cresol Novolak resin) and a sensitizer (diazonaphthoquinone sulfonic ester).[12,20] After irradiation with light in the wavelength range 300–400 nm, photorearrangement and loss of N_2 from the diazoquinone generate an acid that catalyzes the deprotection of a polymeric chain.[20] This process leads to high solubility of the exposed photoresist in an aqueous alkaline solution and results in a positive image [Fig. 1(a)]. The unique structure of the photoactive compound makes it possible, however, to reverse a positive tone to a negative tone in the exposed photoresist by the introduction of a postexposure-bake process to the sequence [Fig. 1(b)]. Postexposure baking provides the reaction conditions necessary to induce acid-catalyzed crosslinking in the exposed regions.[12] The increased molecular weight of the resin in these regions makes it insoluble in aqueous alkali and inert to any further photochemical or thermal processing. The unexposed region is made soluble in the developer by flood-UV exposure. As a result the negative image is produced [Fig. 1(b)].

Figure 2 shows the relation reported previously[12] for the thickness of the AZ 5200 series of photoresist films processed in the conventional and image-reversal modes as a function of the integrated dose of radiation. The values I_0 correspond to the integrated dose of radiation, above which (for positive images) and below which (for negative images) the photoresist film is fully developable. The values I_{100} correspond to the integrated dose of radiation, below which (for positive images) and above which (for negative images) the photoresist film remains intact following development. The $I_0 < I < I_{100}$ interval depicts a so-called clipping level.[2] It is narrower in the image-reversal mode than in the conventional

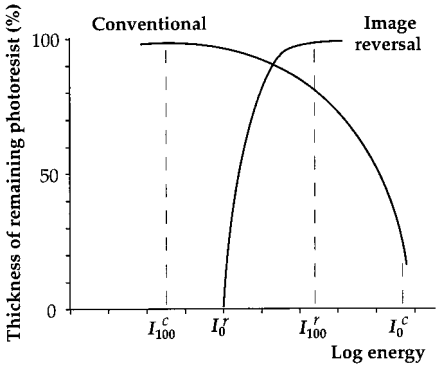

Fig. 2. Depth of the relief in the photoresist processed in conventional and image-reversal modes as a function of the integrated dose of radiation.[12] In the conventional mode the photoresist film is fully developed for energies above $I_0{}^c$ and remains intact for energies below $I_{100}{}^c$. In the image-reversal mode the photoresist film is fully developed for energies below $I_0{}^r$ and remains intact for energies above $I_{100}{}^r$.

mode (Fig. 2), implying higher photosensitivity of the former.

The exposure conditions shown in Fig. 3 illustrate our approach to the experimental design. In a set of controlled experiments we varied the time of exposure of the image-reversal photoresist. The characteristics of exposure were chosen to correspond to the $I_0 < I < I_{100}$ interval [Fig. 3(b)]. For this interval we can derive information about minor differences in the intensity of light from the variations in thickness of

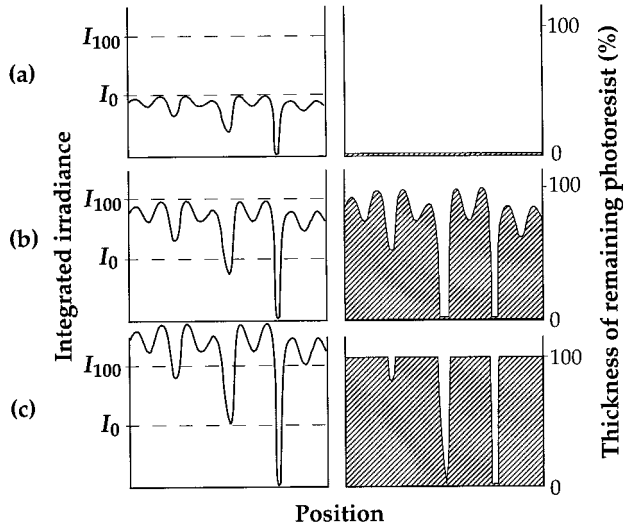

Fig. 3. Relation between an arbitrary intensity profile and corresponding patterns in the image-reversal photoresist as a function of exposure time. (a) Short exposure: when the entire profile of the intensity falls below the level of I_0. The photoresist film is fully developed. (b) Intermediate exposure: when most of the intensity falls into the interval between I_0 and I_{100}. The profile in the photoresist reflects the actual irradiation distribution in the near field. (c) Long exposure: when most of the intensity exceeds the I_{100} level. In the overexposed regions 100% of the photoresist film remains intact irrespective of the actual irradiance distribution.

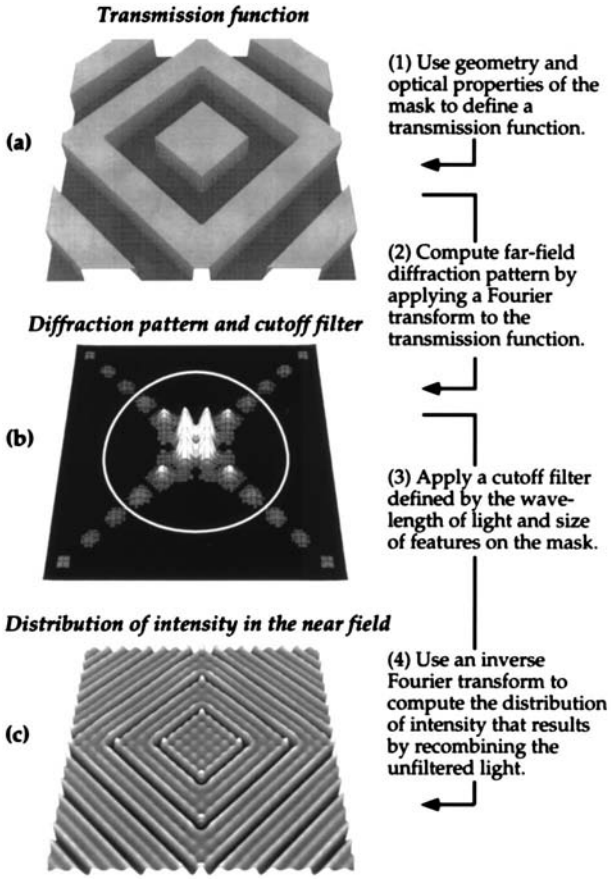

Fig. 4. Steps for computing the near-field pattern of intensity by use of a simple scalar theory. (a) The geometry of the photomask and its optical properties define a transmission function. This function determines the influence of the mask on the phase and amplitude of the light passing through it. For the example illustrated here the mask shifts the phase of the light in a binary fashion. (b) Fourier transformation of the transmission function defines a far-field diffraction pattern. (The amplitude of the electric field is shown here.) The angular positions of diffracted orders in this pattern are determined by (i) the size of features on the mask and (ii) the wavelength of the light evaluated in the medium into which the diffracted light passes after it emerges from the mask. A cutoff filter (dashed white circle) that removes all the diffracted light that emerges from the mask at angles $>90°$ is applied to the pattern of diffraction. (c) The filtered diffracted light is recombined by use of an inverse Fourier transform. The resulting pattern of intensity represents an approximation of the actual pattern in the near field of the mask; it neglects contributions from evanescent waves at the surface of the mask.

the photoresist remaining after development because the percentage of remaining film is almost linearly related to the integrated radiation. This imaging method was used in a study of the irradiance distribution in the near-field photolithographic experiments with an elastomeric phase mask[4–5] in conformal contact with a thin (0.5-μm) film of AZ 5206 photoresist supported on Si/SiO_2.

B. Simulations and Simple Theory

Computations of the near-field patterns of intensity were performed by use of a simple scalar theory de-

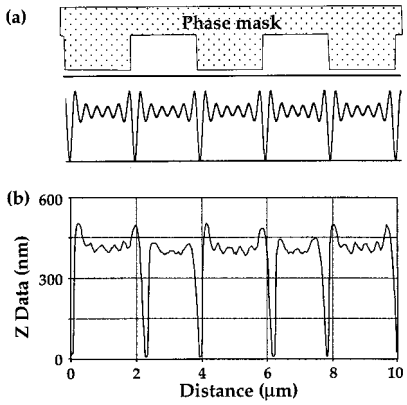

Fig. 5. (a) Theoretical profile of the intensity calculated by use of a simple scalar analysis and (b) AFM height profile of the corresponding pattern recorded in the photoresist for the near-field photolithographic experiment with an elastomeric contact phase mask with a grating test pattern of 2-μm lines spaced by 2 μm.

scribed previously.[5,13,19,21,22] Briefly, the geometry and optical properties of the mask define a transmission function. The transmission function $\tau(x, y)$ is a complex function that determines, according to Eq. (1), how the mask located at $z = 0$ modulates the light that propagates toward positive z and passes through the mask:

$$E(x, y, z = 0^{+}) = E(x, y, z = 0^{-})\tau(x, y). \qquad (1)$$

Fourier transformation of the transmission function yields the far-field diffraction pattern. The diffraction pattern consists of diffracted orders at various angular locations determined by the geometry of the mask, its optical properties, and the index of refraction of the material into which the light propagates after it emerges from the mask. Diffracted beams with angles >90° are evanescent and do not propagate out of the mask. Recombination of diffracted beams with angles <90° determines the pattern of intensity in the near field of the mask, neglecting contributions from evanescent waves.

The procedure for computing the near-field pattern of intensity that neglects these evanescent waves is thus the following: (1) Fourier transformation of the transmission function defines the far-field diffraction pattern; (2) the dimensions of the features on the mask and the wavelength of light, evaluated in the material into which the light propagates, determine the angular locations of the various diffracted beams; (3) filtering of the diffraction pattern removes diffracted beams with angles >90°; (4) inverse Fourier transformation of this filtered diffraction pattern defines the near-field pattern of intensity. Figure 4 illustrates these steps. We performed all computations assuming collimated, monochromatic light. The experiment involved loosely collimated, polychromatic light. The sensitivity of the resist is, however, limited to a narrow range of wavelengths (300–400 nm), making a broadband polychromatic light source effectively monochromatic (365-nm peak) for the purposes of the imaging experiments.

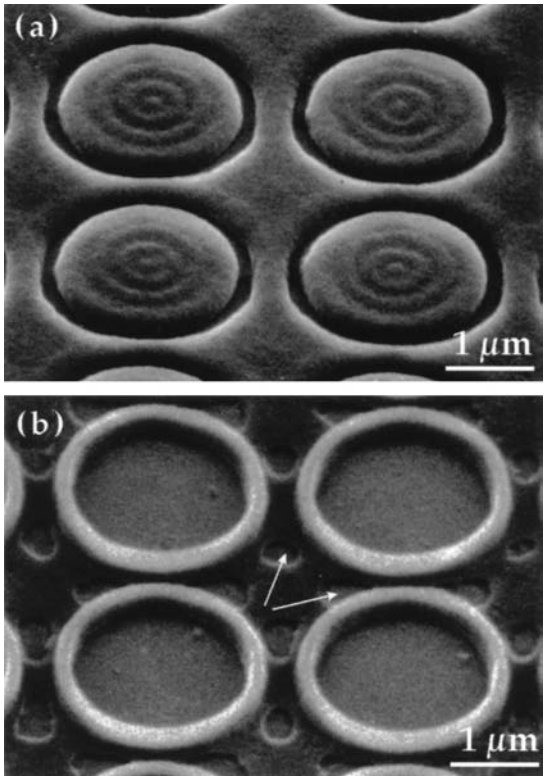

Fig. 6. Scanning electron micrographs of the profiles in the photoresist produced by a phase mask with a relief structure composed of raised cylinders. (a) Image-reversal mode. Diffraction information is recorded inside the circular regions that are in intimate contact with the photoresist. (b) Positive image. Traces of the photoresist film remaining outside the circles (noncontact area in the phase mask) imply that the photoresist accumulates a lower integrated irradiance in the noncontact regions than in the contact regions. Fully developed spots outside the circles (indicated by arrows) correspond to the increased irradiation owing to the interference of peaks in the near-field intensity profiles.

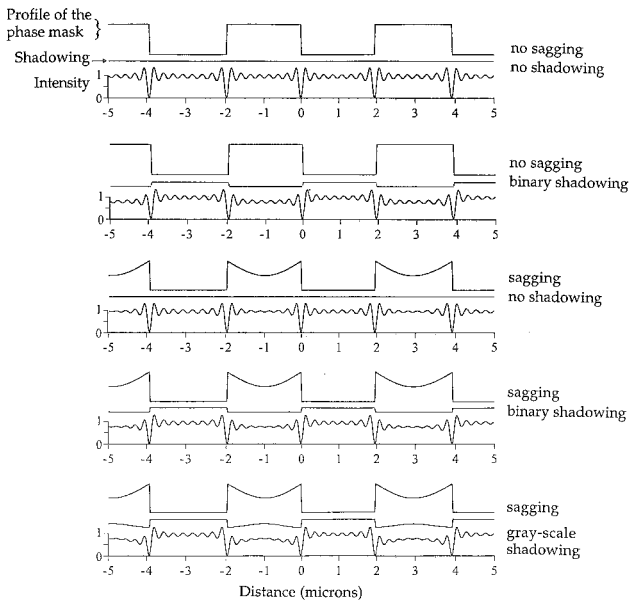

Fig. 7. Theoretical profiles of light intensity corrected for sagging and reflective losses in the noncontact regions of the elastomeric phase mask.

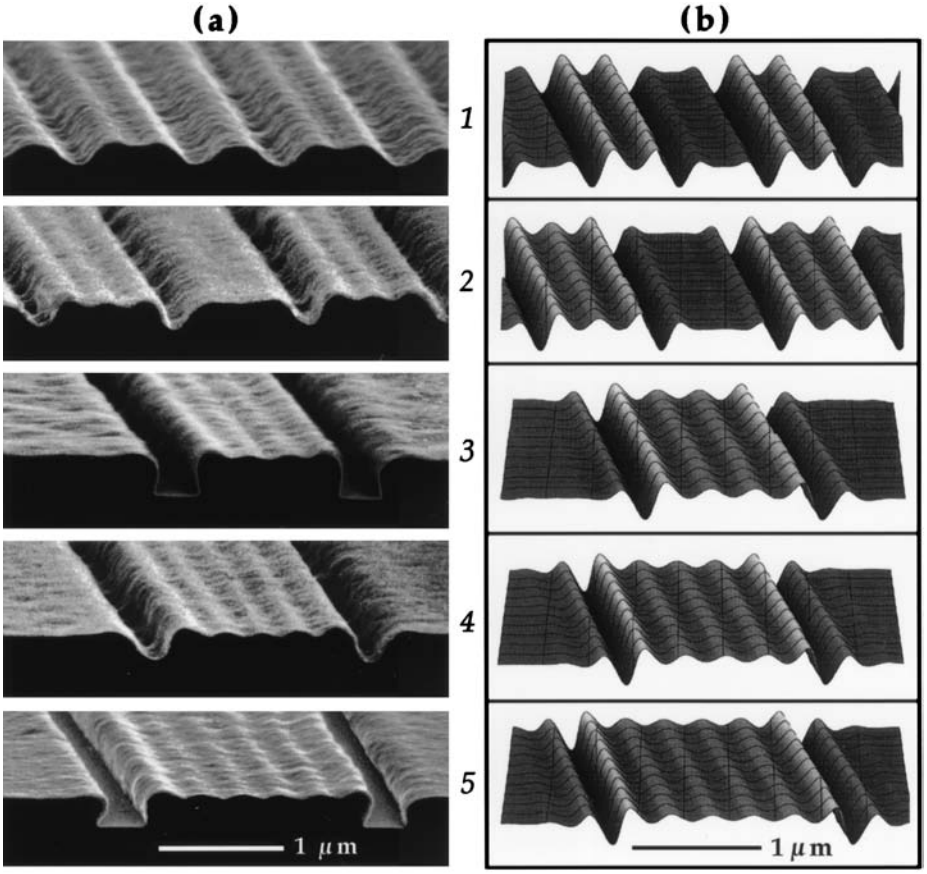

Fig. 8. Near-field irradiance distribution for grating test patterns with different periods p and linewidths w. (a) Scanning electron micrographs of the images of the field recorded in the photoresist. (b) Simulation of the profiles of intensity corrected for sagging and reflective losses at the noncontact regions. *1:* $p = 1600$ nm, $w = 750$ nm. *2:* $p = 2100$ nm, $w = 1000$ nm. *3:* $p = 3500$ nm, $w = 1250$ nm. *4:* $p = 3100$ nm, $w = 1500$ nm. *5:* $p = 3900$ nm, $w = 1900$ nm.

C. Test Patterns and Qualitative Observations

We compare and contrast the calculated profiles of intensity and the patterns in the image-reversal photoresist obtained for a one-dimensional grating test pattern with 2-μm lines separated by 2-μm spaces. The correlation between profiles of intensity calculated by use of a simple scalar analysis [Fig. 5(a)] and profiles for thickness of the photoresist remaining after development measured with an AFM [Fig. 5(b)] establishes that this procedure images the intensity distribution in the near field.

The relative analysis of the theoretical and experimental profiles provides additional information on the distribution of light in the near-field contact-mode lithographic experiments. The ripples in the topology of the photoresist that arise from diffraction appear only between every other deep minimum [Fig. 5(b)], whereas the calculated intensity patterns predict that they should be present in every region [Fig. 5(a)]. In a complementary series of experiments using phase masks where the contact and noncontact regions are geometrically different, we established that the flat areas in the photoresist patterns correspond to the noncontact regions in the mask relief, while the areas bearing the diffraction information correspond to the contact regions. As an example, Fig. 6(a) presents a profile in the image-reversal photoresist produced by a phase mask that had a relief structure composed of raised cylinders with a diameter of 2 μm. A clear diffraction pattern was formed inside the circles (the contact area) but not outside.

Another important observation is that the photoresist accumulates a higher integrated irradiance in the contact regions than in the noncontact regions. This conclusion was based on the profile measurements of the photoresist topology by use of an AFM, showing that the photoresist film is thinner in the areas corresponding to the noncontact regions in the photomask relief than in the contact areas [Fig. 5(b)]. We thus infer that losses in intensity (or shadowing) occur in the noncontact regions relative to the contact regions. Images taken in the photoresist processed in the positive mode show the difference in illumination between the contact and noncontact regions more clearly than do those in the image-reversal mode, and these images confirm that the intensity of light is lower in noncontact than in contact regions [Fig. 6(b)].

D. Factors Contributing to the Deviation in Light Intensity from a Simple Theoretical Model

The deviations of the experimental profiles from their calculated counterparts indicate that theory and ex-

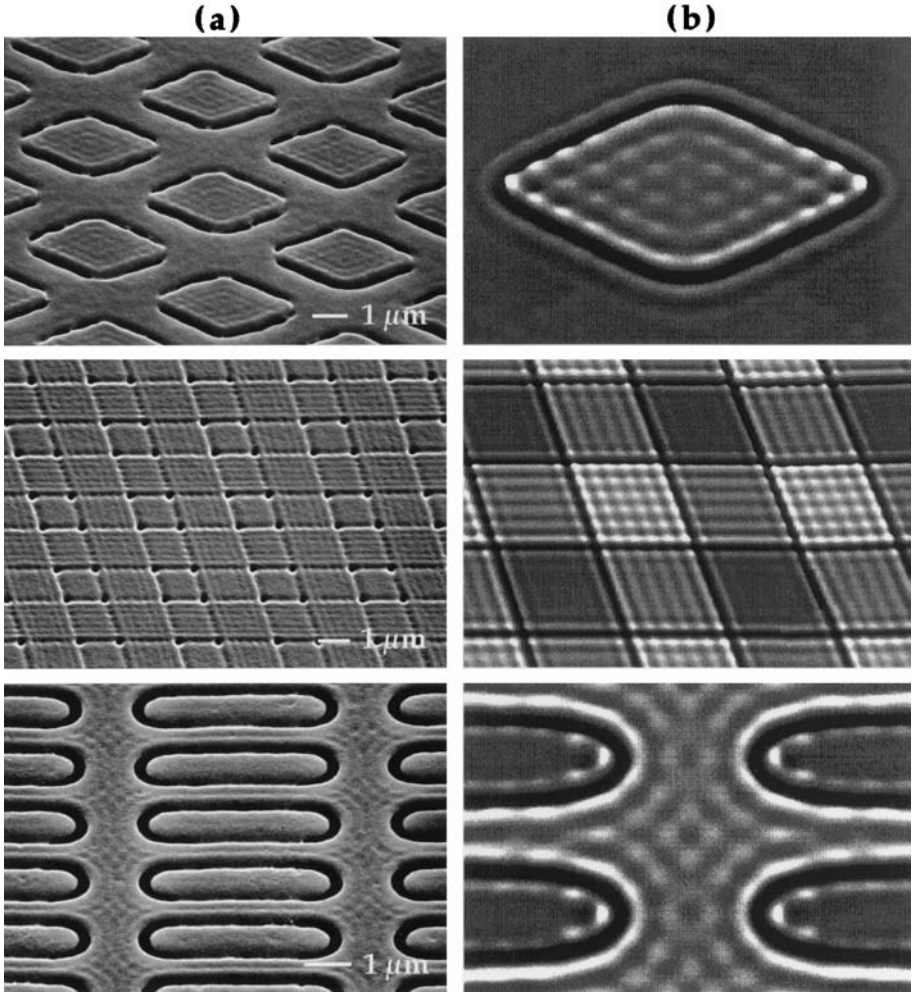

Fig. 9. (a) Scanning electron micrographs of the interference patterns recorded in the photoresist and (b) their theoretical counterparts. The relief structures in the PDMS masks were composed of raised rhombi (top), one-dimensional grating patterns, as in Figs. 3(a) and 5, exposed consecutively in two perpendicular directions (center) and elliptical wells (bottom).

periment agree in the broad features of the system but disagree in important details (for example, the profiles of contact and noncontact regions). This disagreement can result from (i) inappropriate assumptions for theoretical modeling or (ii) an inaccurate description of the experiment, or a combination of both. We believe that (ii) is more important.

In particular, we propose that one source of shadowing observed in our photolithographic experiments is reflective losses in the air gaps that correspond to the raised areas in the mask relief. This conclusion was supported by the AFM measurements of the photoresist profiles obtained by use of elastomeric phase masks with different depths of relief structures: the difference in the thicknesses of the photoresist between noncontact and contact areas decreased with shallower phase masks. Another factor that may contribute to the deviation of the light intensity from a simple theoretical model is the distortion of the elastomeric photomask when it comes in contact with the photoresist, for example, from sagging of the noncontact regions.[23]

To demonstrate the importance of sagging we performed a comparative study of the profiles recorded in the photoresist with PDMS masks of different stiffness or different thickness. In the controlled experiments we established the relation between stiffness (or thickness) and sagging. The masks with grating test patterns and wide (5–10-μm) spaces between lines were brought into conformal contact with the photoresist surface, and the time needed for complete wetting of the surface was measured. This time increased with the increase in stiffness and the decrease in thickness of the masks, suggesting that stiffer or thinner masks supported on a rigid backing exhibit less sagging. Imaging the irradiance distribution with the masks that showed less sagging resulted in the formation of weak diffraction ripples in the noncontact areas, in better agreement with calculations.[5]

E. Imaging the Intensity Profiles

Figure 7 illustrates the correction steps in the theoretical model that account for shadowing from reflective losses and sagging. We used these steps to improve the simulations of the irradiance distribution in the optical near field. Figure 8 shows the

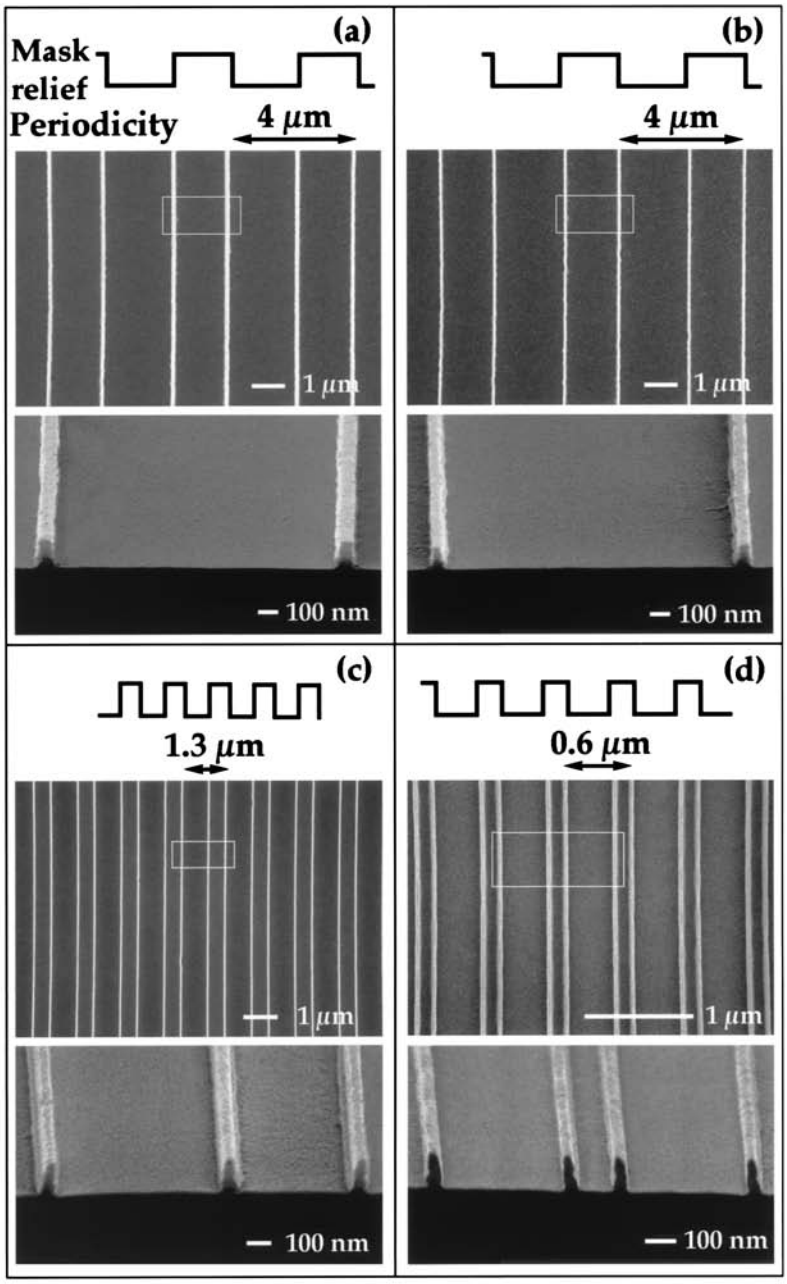

Fig. 10. Scanning electron micrographs of lines in the positive photoresist formed by near-field contact-mode photolithography with (a) a 5-mm-thick, soft elastomeric phase mask having a 500-nm depth of relief, as described previously,[4,5] and (b)–(d), a 2-mm-thick, stiff elastomeric phase mask having a 300-nm depth of relief. The periodicity in the mask relief decreases from (b) to (d).

reconstructed profiles of intensity produced by elastomeric phase masks that have grating test patterns with different periods p and linewidths w. These profiles are remarkably similar to the corresponding patterns recorded in the photoresist. The sensitivity of the proposed imaging method extends to more complex interference patterns. Figure 9 presents sample profiles in the photoresist and the corresponding calculated distributions of intensity.

It is clear that the images in the photoresist provide detailed information of the three-dimensional distribution of intensity of light in the optical near field. The simple scalar calculations, neglecting contributions from evanescent waves, account for essentially all the features in the experimental profiles. We can therefore conclude that the distribution of intensity is defined primarily by the geometry and optical properties of the mask, whereas the contributions from the evanescent waves are negligible compared with the resolution of the photoresist (~20 nm).

F. Application of the Technique

Our results suggest that one can improve the quality of features generated by near-field contact-mode photolithography with elastomeric contact phase masks

by (i) decreasing sagging of the mask by increasing the stiffness and decreasing the thickness of the mask and (ii) reducing shadowing in the air gap by partially decreasing the depth of the relief structure in the mask without significantly decreasing the phase contrast.

We generated patterns in the positive photoresist using elastomeric phase masks that had been prepared as described previously[4,5] {PDMS, 10:1 (see Section 2 for details); thickness, 5 mm; depth of the relief, 500 nm [Fig. 10(a)]} and that had been optimized according to procedures (i) and (ii) {PDMS, 6:1; thickness, 2 mm; depth of the relief, 300 nm [Fig. 10(b)]}. The widths of the photoresist lines obtained after development were ~100 and ~70 nm for nonoptimized and optimized masks, respectively. A further decrease in the linewidths was attained by use of optimized PDMS phase masks with increased density of the features, as predicted[5] [Figs. 10(c) and 10(d)]. Lines in the photoresist as small as 50 nm were formed. We believe that the linewidth is limited mostly by the granularity of the photoresist (~20–30 nm as estimated from the AFM images) and that the potential of near-field conformal-contact photolithography can be extended to the successful fabrication of features with linewidths below 50 nm by use of high-resolution photoresists.

4. Conclusions

Redistribution of intensity is an important concern in the realization of nanostructures by use of near-field photolithography. The capability of the imaging technique based on uses of a sensitive negative-tone photoresist to characterize the irradiance directly provides a new tool for understanding the principles of near-field photolithography. This knowledge will make it possible to improve both existing theoretical models and experimental practice. The analysis of the near-field images highlights issues in the experimental design, provides a means for their optimization, and extends the application of near-field conformal-contact photolithography to the deep sub-100-nm range.

This study was supported in part by the Office of Naval Research, the Defense Advanced Research Projects Agency, and the National Science Foundation (PHY-9312572). J. A. Rogers acknowledges support from the Harvard University Society of Fellows. We thank L. Goetting and S. Shepard for their assistance in using the AFM and the photolithographic facilities.

References

1. H. I. Smith, "A review of submicron lithography," Superlat. Microstruct. **2,** 129–142 (1986).
2. H. I. Smith, N. Efremow, and P. L. Kelley, "Photolithographic contact printing of 4000 Å linewidth patterns," J. Electrochem. Soc. **121,** 1503–1506 (1974).
3. F. Cerrina and C. Marrian, "A path to nanolithography," MRS Bull. **12,** 56–61 (1996).
4. J. A. Rogers, K. E. Paul, R. J. Jackman, and G. M. Whitesides, "Using an elastomeric phase mask for sub-100 nm photolithography in the optical near field," Appl. Phys. Lett. **70,** 2658–2660 (1997).
5. J. A. Rogers, K. E. Paul, R. J. Jackman, and G. M. Whitesides, "Generating ~90 nanometer features using near-field contact-mode photolithography with an elastomeric phase mask," J. Vac. Sci. Technol. (in press).
6. B. J. Lin, "Optical methods for fine line lithography," in *Fine Line Lithography*, R. Newman, ed. (Elsevier, North Holland, 1980), pp. 105–232.
7. B. J. Lin, "Near-field diffraction of a medium slit," J. Opt. Soc. Am. **62,** 977–981 (1972).
8. B. J. Lin, "Deep-UV conformable-contact photolithography for bubble circuits," IBM J. Res. Dev. **20,** 213–221 (1976).
9. S. Davy and M. Spajer, "Near field optics: snapshot of the field emitted by a nanosource using a photosensitive polymer," Appl. Phys. Lett. **69,** 3306–3308 (1996).
10. L. Mashev and S. Tonchev, "Formation of holographic diffraction gratings in photoresist," Appl. Phys. A **26,** 143–147 (1981).
11. G. C. Bjorklund, S. E. Harris, and J. F. Young, "Vacuum ultraviolet holography," Appl. Phys. Lett. **25,** 451–453 (1974).
12. M. Spak, D. Mammato, S. Jain, and D. Durham, "Mechanism and lithographic evaluation of image reversal in AZ 5214 photoresist," presented at the Seventh International Technical Conference on Photopolymers, Ellenville, New York, 1985.
13. M. Levenson, "Wavefront engineering for photolithography," Phys. Today **7,** 28–36 (1993).
14. J. C. Langston and G. T. Dao, "Extending optical lithography to 0.25 μm and below," Solid State Technol. **3,** 57–64 (1995).
15. K. O. Hill, B. Malo, F. Bilodeau, D. C. Johnson, and J. Albert, "Bragg gratings fabricated in monomode photosensitive optical fiber by UV exposure through a phase mask," Appl. Phys. Lett. **62,** 1035–1037 (1993).
16. T. Tanaka, S. Uchino, N. Hasegawa, T. Yamanaka, T. Terasawa, and S. Okazaki, "A novel optical lithography technique using the phase-shifter fringe," Jpn. J. Appl. Phys. **30**(5), 1131–1136 (1991).
17. P. Brock, M. D. Levenson, J. M. Savislan, J. R. Lyerla, J. C. Cheng, and C. V. Podlogar, "Fabrication of grooved glass substrates by phase mask lithography," J. Vac. Sci. Technol. B **9**(6), 3155–3161 (1991).
18. A. Kumar and G. M. Whitesides, "Features of gold having micrometer to centimeter dimensions can be formed through a combination of stamping with an elastomeric stamp and an alkanethiol 'ink' followed by chemical etching," Appl. Phys. Lett. **63,** 2002–2005 (1993).
19. M. V. Klein, *Optics* (John Wiley & Sons, New York, 1970).
20. A. Reiser, H.-Y. Shih, T.-F. Yeh, and J.-P. Huang, "Novolak-diazoquinone resists: the imaging systems of the computer chip," Angew. Chem. Int. Ed. Engl. **35,** 2428–2440 (1996).
21. J. W. Goodman, *Introduction to Fourier Optics* (Pergamon Press, New York, 1980).
22. P. E. Dyer, R. J. Farley, and R. Geidl, "Analysis of grating formation with excimer laser irradiated phase masks," Opt. Commun. **115**(3-4), 323–334 (1995).
23. E. Delamarche, H. Schmid, B. Michel, and H. Biebuyck, "Stability of molded polydimethylsiloxane microstructures," Adv. Mater. **9,** 741–746 (1997).